ELSEVIER

Experimental Hematology

Experimental Hematology 2018;00:00-00

Mesenchymal stromal cells induce a permissive state in the bone marrow that enhances G-CSF-induced hematopoietic stem cell mobilization in mice

Evert-Jan F.M. de Kruijf, Rob Zuijderduijn, Marjolein C. Stip, Willem E. Fibbe, and Melissa van Pel

Department of Immunohematology and Blood Transfusion, Leiden University Medical Center, Leiden, The Netherlands

(Received 12 March 2018; revised 17 April 2018; accepted 8 May 2018)

Mesenchymal stromal cells (MSCs) support hematopoietic stem cells (HSCs) in vivo and enhance HSC engraftment and hematopoietic recovery upon cotransplantation with HSCs. These data have led to the hypothesis that MSCs may affect the HSC niche, leading to changes in HSC retention and trafficking. We studied the effect of MSC administration on the HSC compartment in the bone marrow (BM) in mice. After injection of MSCs, HSC numbers in the BM were decreased coinciding with an increased cell cycle activity compared with phosphate-buffered saline (PBS)-injected controls. Furthermore, the frequency of macrophages was significantly reduced and niche factors including *Cxcl12*, *Scf*, and *Vcam* were downregulated in endosteal cells. These BM changes are reminiscent of events associated with granulocyte colony-stimulating factor (G-CSF)-induced hematopoietic stem and progenitor cell (HSPC) mobilization. Interestingly, coadministration of MSCs and G-CSF resulted in a twofold increase in peripheral blood HSPC release compared with injection of G-CSF alone, whereas injection of MSCs alone did not induce HSPC mobilization. After intravenous administration, MSCs were only observed in the lungs, suggesting that they exert their effect on the HSC niche through a soluble mediator. Therefore, we tested the hypothesis that MSC-derived extracellular vesicles (EVs) are responsible for the observed changes in the HSC niche. Indeed, administration of EVs resulted in downregulation of *Cxcl12*, *Scf*, and *Vcam* and enhanced G-CSF-induced HSPC mobilization at similar levels as MSCs and G-CSF. Together, these data indicate that MSCs induce a permissive state in the BM, enhancing HSPC mobilization through the release of EVs.

Hematopoietic stem cells (HSCs) replenish the peripheral blood (PB) cell pool throughout life. During homeostasis, the vast majority of HSCs reside in specialized niches located in the perivascular area of the trabeculated region of the bone marrow (BM). This HSC microenvironment regulates self-renewal, cell cycle entry, and differentiation of HSCs and consists of a complex network of hematopoietic and nonhematopoietic cells (see previous reviews [1,2]).

In the BM, the majority of HSCs are found in close proximity to mesenchymal stromal cells (MSCs) surrounding arterioles and sinusoids [3–6]. MSC-derived CXCL12 and stem cell factor (SCF) are indispensable for HSC maintenance because deletion of either CXCL12 or SCF leads to hematopoietic exhaustion [7–11]. HSCs are retained in the niche by adhesion molecules, including β1-integrins, interacting with extracellular matrix components and with vascular cell adhesion molecule (VCAM), which is expressed on stromal cells [12].

The endosteal region of the BM contains a population of resident macrophages (osteal macrophages or

Offprint requests to: M. van Pel, Ph.D., Department of Immunohematology and Blood Transfusion, Leiden University Medical Center, P.O. Box 9600, 2300 RC Leiden, The Netherlands; E-mail: m.van_pel@lumc.nl

Supplementary material associated with this article can be found, in the online version, at doi:10.1016/j.exphem.2018.05.002.

https://doi.org/10.1016/j.exphem.2018.05.002

osteomacs) supporting osteoblast differentiation and mineralization and contributing to the maintenance of HSC niches [13]. Another BM-resident macrophage population, expressing CD169, supports the retention of HSCs by acting on stromal cells in the niche [15]. Depletion of osteomacs or $CD169^+$ macrophages results in downregulation of *Cxcl12*, *Vcam, Ang-1*, and *Scf* and results in subsequent hematopoietic stem and progenitor cell (HSPC) mobilization [13–15].

Through administration of exogenous cytokines, HSPCs can be induced to leave the niche and migrate toward the PB in a process called mobilization. Granulocyte-colony stimulating factor (G-CSF) is most commonly applied as a mobilizing agent.

The administration of G-CSF is accompanied by neutrophil expansion and a proteolytic BM milieu coinciding with decreased levels of the protease inhibitor alpha-1-antitrypsin (AAT) [16,17]. Simultaneously with neutrophil expansion, G-CSF administration leads to depletion of macrophages, resulting in decreased expression of *Cxcl12*, *Vcam*, and *Scf* by BM stromal cells and in decreased osteoblast numbers [14,15]. Together, these events result in decreased adhesion of HSPCs to their niche and, as a consequence, HSPCs migrate toward the PB.

MSCs are a nonhematopoietic population of cells that form fibroblast colony-forming units and have the capacity to differentiate into osteoblasts, adipocytes, and chondrocytes. MSCs can be isolated from the BM, where they are an essential part of the HSC niche [2]. When cotransplanted with $CD34^+$ umbilical cord blood-derived HSPCs, MSCs enhance both HSC engraftment and hematopoietic recovery [18,19]. Although the underlying mechanisms are not fully understood, it was suggested that HSC homeostasis is altered indirectly through factors released by the injected MSCs because intravenously injected MSCs could not be detected in the BM after administration [19].

Given the key role of MSCs in the HSC microenvironment and their effect on HSC engraftment and hematopoietic recovery, we have investigated the effect of MSC administration on the hematopoietic BM compartment. Here, we show that intravenous administration of MSCs results in changes in the BM that are reminiscent of events that occur during G-CSF-induced HSPC mobilization. Furthermore, coinjection of MSCs and G-CSF synergistically enhanced HSPC mobilization compared with G-CSF alone. MSCs retained in the lung exerted their effects on the BM through the secretion of extracellular vesicles (EVs). Administration of EVs alone resulted in downregulation of *Cxcl12*, *Scf*, and *Vcam* and enhanced G-CSF-induced HSPC mobilization at similar levels as MSCs. Together, these data indicate that MSC administration induces a permissive state in the BM through the release of EVs, promoting HSPC mobilization.

Methods

Animals

Eight- to 12-week-old male C57BL/6-Ly5.2 and C57BL/6-Ly5.1 mice were obtained from Charles River Laboratories (Maastricht, The Netherlands). The animals were fed commercial rodent chow and acidified water ad libitum and were maintained in the animal facility of the Leiden University Medical Center (LUMC) under conventional conditions. All experimental protocols were approved by the institutional ethics committee on animal experiments.

Mesenchymal stromal cells

MSCs were obtained by culturing bone chips in a 75 cm^2 flask in MSC medium containing α-minimum essential medium (Life Technologies), 10% fetal calf serum (FCS), penicillin/streptomycin, and L-glutamine. Plastic adherent MSCs were cultured to 95% confluency in a fully humidified atmosphere at 37°C and 5% CO_2, harvested using trypsin, and further expanded until sufficient numbers were obtained. MSCs used throughout this study were of passage six to ten. MSCs were administered intravenously in 0.1% bovine serum albumin/PBS (0.1% BSA/PBS) at a dose of 200×10^3 cells per day for 3 consecutive days. Mice injected with 0.1% BSA/PBS served as controls. In indicated experiments, MSCs were cultured in the presence of recombinant murine interferon-gamma (IFN-γ) (20 ng/mL) or recombinant murine tumor necrosis factor-alpha (TNF-α) (20 ng/mL; both R&D Systems, Abingdon, UK) for 7 days. Where indicated, MSCs were transduced with a lentiviral vector containing *SFFV-DsRed-Firefly luciferase (SFFV-DsR-Fluc)* as described previously [21]. Images were acquired and analyzed as described previously [21]. To obtain MSC culture supernatant, MSCs at a confluency of 70–80% were cultured for 1 week in StemSpan (STEMCELL Technologies, Köln, Germany). Subsequently, the medium was harvested, centrifuged to deplete for cell debris, and concentrated using Centriprep YM3 filters (Millipore, Amsterdam, the Netherlands) to obtain an ~20-fold concentration. In indicated experiments, 200 μL of MSC culture supernatant was administered intraperitoneally twice daily for 3 consecutive days.

Cell lines

RAW264.7 cells (gift from A. van Wengen, LUMC) were cultured in RPMI-1640 medium containing 10% FCS, penicillin, streptomycin and L-glutamine. S17 and MS-5 cells (gift from F.J.T. Staal, LUMC) were cultured in MSC medium and MSC medium with 50 μmol/L 2-mercaptoethanol (Sigma-Aldrich, Zwijndrecht, The Netherlands), respectively.

In coculture experiments, 35×10^3 stromal cells were cultured in their respective medium for 16 hours and then medium was removed and RAW264.7 cells were added in a 1:1 ratio and cultured for 72 hours in MSC medium. RAW264.7 cells were either added directly to the stromal cells or cultured in Transwells with a 0.4 μm pore size

(Corning Costar). Stromal cells were harvested using Accumax (eBioscience). RAW264.7 cells were depleted using CD45 microbeads (Miltenyi, Leiden, The Netherlands) and MACS separation.

Preparation of cell suspensions and BM extracellular extracts

Twenty-two to 24 hours after the last MSC administration, mice were sacrificed by CO_2 asphyxiation. PB was obtained by intracardiac puncture and cell counts were performed on a Sysmex XP-300 counter (Sysmex, Etten-Leur, The Netherlands). PB was centrifuged at 350 *g* and blood plasma was stored at −20°C. Erythrocytes were lysed using a specific lysis buffer (LUMC Pharmacy, Leiden, The Netherlands) before further analysis. BM and spleen cells were harvested as described previously [22].

BM extracellular extracts were obtained by flushing femurs with 250 μL of cold PBS. The cell suspension was centrifuged at 350 *g* for 7 minutes at 4°C. The supernatant was stored at −20°C.

To enumerate osteoclasts, 1×10^5 BM cells were seeded in quintuplicate in a 96-well flat-bottomed plate and stained using the tartrate-resistant acid phosphatase (TRAP) staining kit (Sigma-Aldrich) according to the manufacturer's recommendations.

Antibodies for cell analysis

All antibodies used are described in Table 1. Cells were analyzed on a FACSCanto II flow cytometer with Diva software (BD Biosciences, Erebodegem, Belgium).

5-Fluorouracil

5-Fluorouracil (5-FU, F6627, Sigma-Aldrich) was dissolved in PBS and administered at a concentration of 150 mg/kg intraperitoneally. Cell recovery was determined every 2−3 days, but individual mice were only bled weekly to avoid excessive stress. A small volume of blood was drawn from the tail vein. Cell counts were performed on a Sysmex XP-300 counter. After lysis of erythrocytes, cells were stained with CD11b-, Ly6G-, BB20-, CD3-, and Ly6C-specific antibodies (Table 1).

Quantitative real-time polymerase chain reaction

After obtaining BM cells by flushing the femurs, the same femurs were flushed with PBS and RLT buffer (Qiagen) to obtain cell lysates of endosteal cells. RNA was obtained using the RNeasy mini kit (Qiagen) according to the manufacturer's recommendations and cDNA was generated using Superscript III (Invitrogen). Primer sets used for quantitative real-time polymerase chain reaction (qRT-PCR) experiments are shown in Table 2. qRT-PCR was performed using TaqMan Universal MasterMix (Thermo Fisher) and Universal Probes (Roche) on a StepOnePlus cycler (Thermo Fisher). Relative gene expression was calculated using the comparative threshold cycle (C_T) method, with *Hprt*, *Abl*, or *Gapdh* as the endogenous reference genes.

Administration of recombinant human G-CSF

Mice were injected intraperitoneally with 10 μg of recombinant human G-CSF (Amgen, Thousand Oaks, California, USA) in 0.2 mL of 0.1 % BSA/PBS once a day for 3 consecutive days. Control mice received 0.2 mL of 0.1% BSA/PBS.

Table 1. Overview of the antibodies used in the study

Antibody	Label	Clone	Company
B220	Fitc, PerCP-Cy5.5	RA3-6B2	BD Pharmingen
CD3	Fitc	145-2C11	BD Pharmingen
CD3	eFluor450	145-2C11	eBioscience
CD4	Fitc	GK1.5	BD Pharmingen
CD8	Fitc	53-6.7	BD Pharmingen
CD11b	biotin, Fitc	M1/70	BD Pharmingen
CD34	Alexa Fluor 647	RAM34	BD Pharmingen
CD45.1	PE, FITC	A20	BD Pharmingen
CD45.2	PerCpCy5.5, Fitc	104	BD Pharmingen
CD68	PerCP-Cy5.5	FA-11	BioLegend
CD115	BV421	AFS98	BioLegend
CD117	APC-eFluor 780	2B8	eBioscience
CD117	PE	2B8	BD Pharmingen
CD135	PE	A2F10.1	BD Pharmingen
CD169	PE	3D6.112	BioLegend
F4/80	Fitc, BV510	BM8	BioLegend
Gr-1	APC, Fitc	RB6-8C5	BD Pharmingen
Ly6C	APC-Cy7	AL-21	BD Pharmingen
Ly6G	APC	1A8	BD Pharmingen
Sca-1	PerCP-Cy5.5	D7	eBioscience
MERTK	PE-Cy7	DS5MMER	eBioscience
TER119	Fitc	TER-119	BD Pharmingen
Ki67	PE-Cy7	B56	BD Pharmingen
Isotype for Ki67	PE-Cy7	IgG1κ	BD Pharmingen
Streptavidin	Pacific Orange	-	Invitrogen

Table 2. Overview of the primer pairs used in the study

Gene	Forward (5′−3′)	Reverse (5′−3′)
HPRT	GGAGCGGTAGCACCTCCT	AACCTGGTTCATCATCGCTAA
GAPDH	AAGAGGGATGCTGCCCTTA	TTGTCTACGGGACGAGGAAA
ABL	TGGAGATAACACTCTAAGCATAACTAAAGGT	GATGTAGTTGCTTGGGACCCA
CXCL12	CTGTGCCCTTCAGATTGTTG	CTCTGCGCCCCTTGTTTA
VCAM-1	TCTTACCTGTGCGCTGTGAC	ACTGGATCTTCAGGGAATGAGT
SCF	TCAACATTAGGTCCCGAGAAA	ACTGCTACTGCTGTCATTCCTAAG
Angpt1	GGAAGATGGAAGCCTGGAT	ACCAGAGGGATTCCCAAAAC
IL-7	CTGCTGCAGTCCCAGTCAT	TCAGTGGAGGAATTCCAAAGA
CSF3R	CTCGACCCCATGGATGTT	GAGAGACTACATCAGGGCCAAT

Progenitor cell assays

Two hundred microliters of PB was depleted of erythrocytes using a specific lysis buffer (LUMC Pharmacy). Next, the equivalent of 100 μL of PB was cultured in duplo in 3.5 cm dishes containing semisolid medium supplemented with recombinant murine GM-CSF (1.25 ng/mL; BD Biosciences), recombinant murine interleukin-3 (IL-3) (25 ng/mL; BD-Biosciences), recombinant human erythropoietin (0.2 units/mL; LUMC Pharmacy), and recombinant human G-CSF (100 ng/mL; Amgen). After 6 days of culture, the number of colonies (defined as an aggregate of $\geq$20 cells) was scored using an inverted light microscope.

PB cell transplantations

Recipients were irradiated in Perspex chambers using an Orthovolt (Xstrahl Medical, Walsall, UK). A total dose of 9.5 Gy total body irradiation (TBI) was administered. Four hours after TBI, 750×10^3 PB mononuclear cells were injected via caudal vein injection in 200 μL of 0.1% BSA/PBS.

Osteoprotegerin and M-CSF

Recombinant murine osteoprotegerin (OPG) was obtained from R&D Systems (Minneapolis, USA), dissolved in PBS, and administered intravenously before G-CSF administration. The OPG concentration was determined using a mouse OPG immunoassay (R&D Systems) according to the manufacturer's recommendations. M-CSF concentrations were assessed using a mouse M-CSF ELISA (R&D Systems).

EVs

EV-depleted MSC medium was obtained by centrifuging MSC medium at 100,000 *g* at 4°C for 16 hours using a Beckman Coulter Ultracentrifuge. MSCs were cultured for 72 hours in EV-depleted medium. Culture supernatant was sequentially centrifuged at 350 *g* for 10 minutes and at 10,000 *g* for 30 minutes to discard cell debris. Supernatant was collected and centrifuged for 70 minutes at 100,000 *g*. The pellet containing EVs was washed in PBS for 70 minutes at 100,000 *g* and resuspended in PBS. EVs were quantified using a qNano particle analyzer (Izon Science, Oxford, UK). EV preparations had a mean particle diameter of 133.7 $\pm$ 3.2 nm. Typically, $5.3 \times 10^{10} \pm 1.7 \times 10^{10}$ EVs were isolated per 1×10^6 MSCs after 3 days of culture. Where indicated, EVs were stained in diluent C solution for 10 minutes using a PKH26 kit (Sigma-Aldrich). Staining was stopped by adding 1% BSA/PBS. Next, EVs were washed for 70 minutes at 100,000 *g* and resuspended in PBS.

Statistical analysis

All values are presented as mean with standard error of the mean. All groups were compared using the unpaired *t* test with Welch's correction when applicable. All statistical calculations were performed using GraphPad Prism software (La Jolla, California, USA). $p \leq 0.05$ was considered statistically significant.

Results

MSC administration increases HSPC cycle activity

To investigate the effect of MSC administration on the hematopoietic compartment in the BM, cohorts of C57BL/6 mice received three consecutive daily injections of MSCs. On day 4, mice were sacrificed and BM cells were analyzed. The absolute number of HSCs (defined as $Lin^-Sca\text{-}1^+c\text{-}Kit^{HI}$ [LSK] $CD34^-CD135^-$) was significantly decreased (Figure 1D), whereas the total number of white blood cells (WBCs) per femur and the colony-forming capacity of the BM remained comparable to controls (Figures 1A and 1B). Moreover, there was a trend toward decreased numbers of LSK cells, hematopoietic progenitor cells (HPCs), and MPPs per femur (Figures 1C−1F). To investigate whether the decrease in HSC numbers was due to altered cell cycle activity of HSPCs, the cell cycle status of the hematopoietic cells after MSC administration was assessed. The frequency of LSK cells in the G_1 phase of cell cycle was a 3.2-fold increase compared with PBS-treated controls, whereas the frequencies of LSK cells in the G_0 and the $S/G_2/M$ phase were decreased with 64% and 50.7% of PBS controls (Figure 1G). A similar shift in cell cycle activity was observed for HSCs and HPCs/MPPs (Supplementary Figures E1A and E1B, online only, available at www.exphem.org). The cytoreductive agent 5-FU kills actively cycling cells, including cycling HSPCs, and induces a BM stress response. In the PB, WBCs were decreased within days after 5-FU injection (Figures 1H and 1I). Administration of MSCs for 3 consecutive days followed by 5-FU injection delayed WBC recovery compared with controls receiving PBS and 5-FU. This delay was even more pronounced in the granulocytic

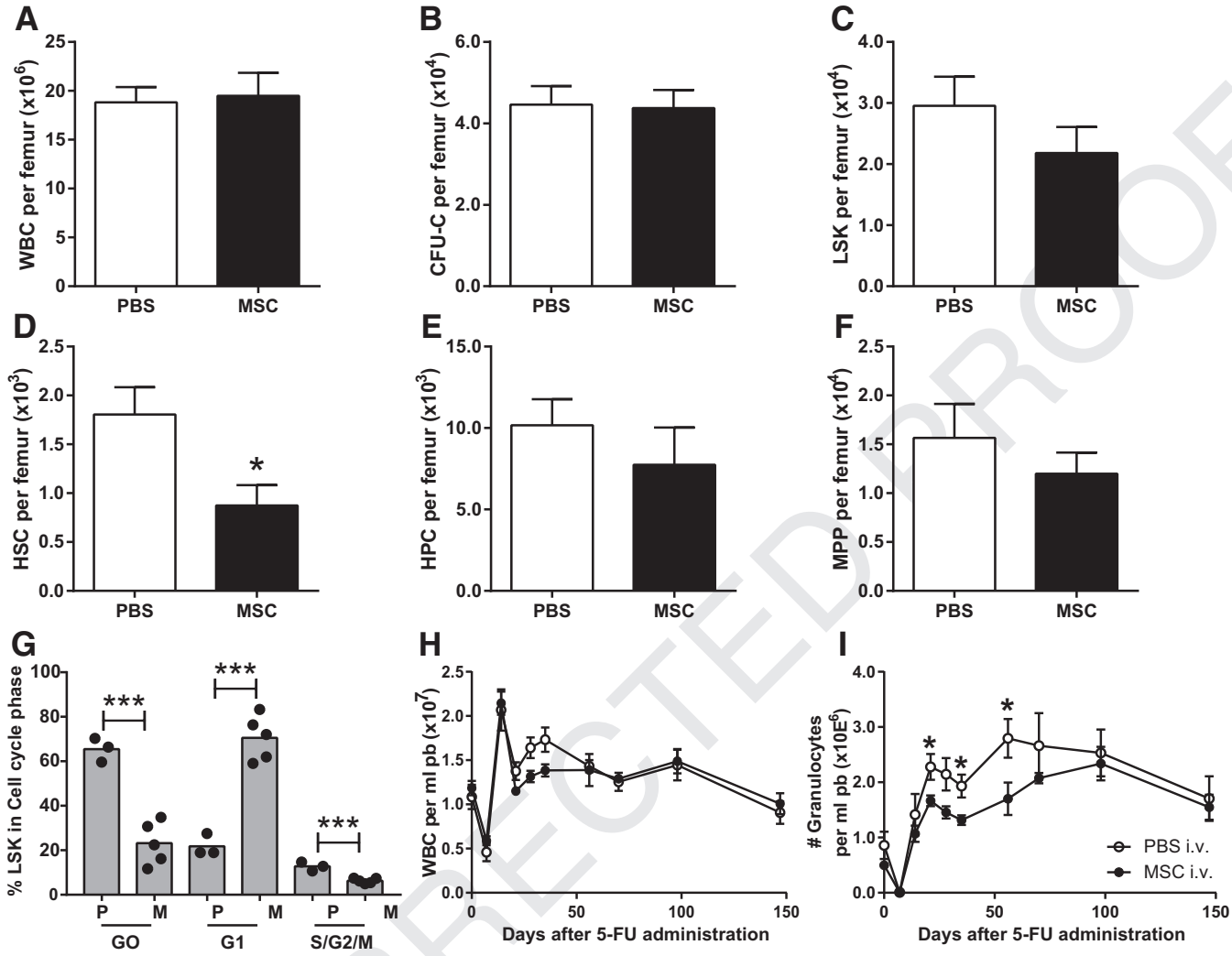

Figure 1. MSC administration increases HSPC cell cycle activity. After 3 days of intravenous MSC or PBS administration, femurs were isolated and analyzed for (A) total WBC numbers and (B) the number of colony-forming cells (CFU-C); $n = 6-8$ per group. (C–F) The absolute number of LSKs, HSCs, HPCs, and MPPs per femur was determined by fluorescence-activated cell sorting analysis; $n = 6$ per group. (G) Cell cycle activity of LSK cells was analyzed using a Ki67/DAPI staining. The frequencies of LSK cells in G_0, G_1, or $S/G_2/M$ phase was determined using flow cytometry. (H,I) After 3 daily intravenous injections of MSCs, mice received 5-FU at a dose of 150 mg/kg (day 0); WBCs per milliliter of PB (H) and the absolute number of granulocytes per milliliter of PB (I) were determined at weekly intervals after 5-FU administration ($n = 5$ per group). Data are depicted as mean ± standard error of the mean of two separate experiments. $^*p < 0.05$, $^{**}p < 0.01$, $^{***}p < 0.001$ all compared with PBS.

compartment (Figures 1H and 1I). Together, these results indicate that administration of MSCs leads to a reduction of the number of LSK cells in the BM and induces HSPCs into the cell cycle.

MSCs downregulate niche factors in the BM

The HSC niche regulates HSC cell cycle entry. Therefore, the observed increase in cell cycle activity of HSPCs after MSC administration may be explained by changes in the niche. Macrophages have been shown to contribute to anchoring HSCs in the niche and their depletion leads to downregulation of HSC retention factors including CXCL12 and VCAM in stromal cells and their depletion induced HSPC mobilization [14,15]. In turn, MSCs act on cells of the innate immune system, including macrophages [23–25]. For these reasons, we hypothesized that MSCs may alter the HSC niche through macrophages as intermediate cells. Therefore, the presence of osteomacs and $CD169^+$ macrophages was assessed in BM after MSC administration. A significant decrease in osteomacs and $CD169^+$ macrophages was observed compared with PBS-injected controls (Figures 2A–2F). Moreover, osteoclasts, which are macrophages specialized in regulating bone metabolism, were also decreased ($p = 0.057$; Figure 2G). The decline in osteoclasts upon MSC

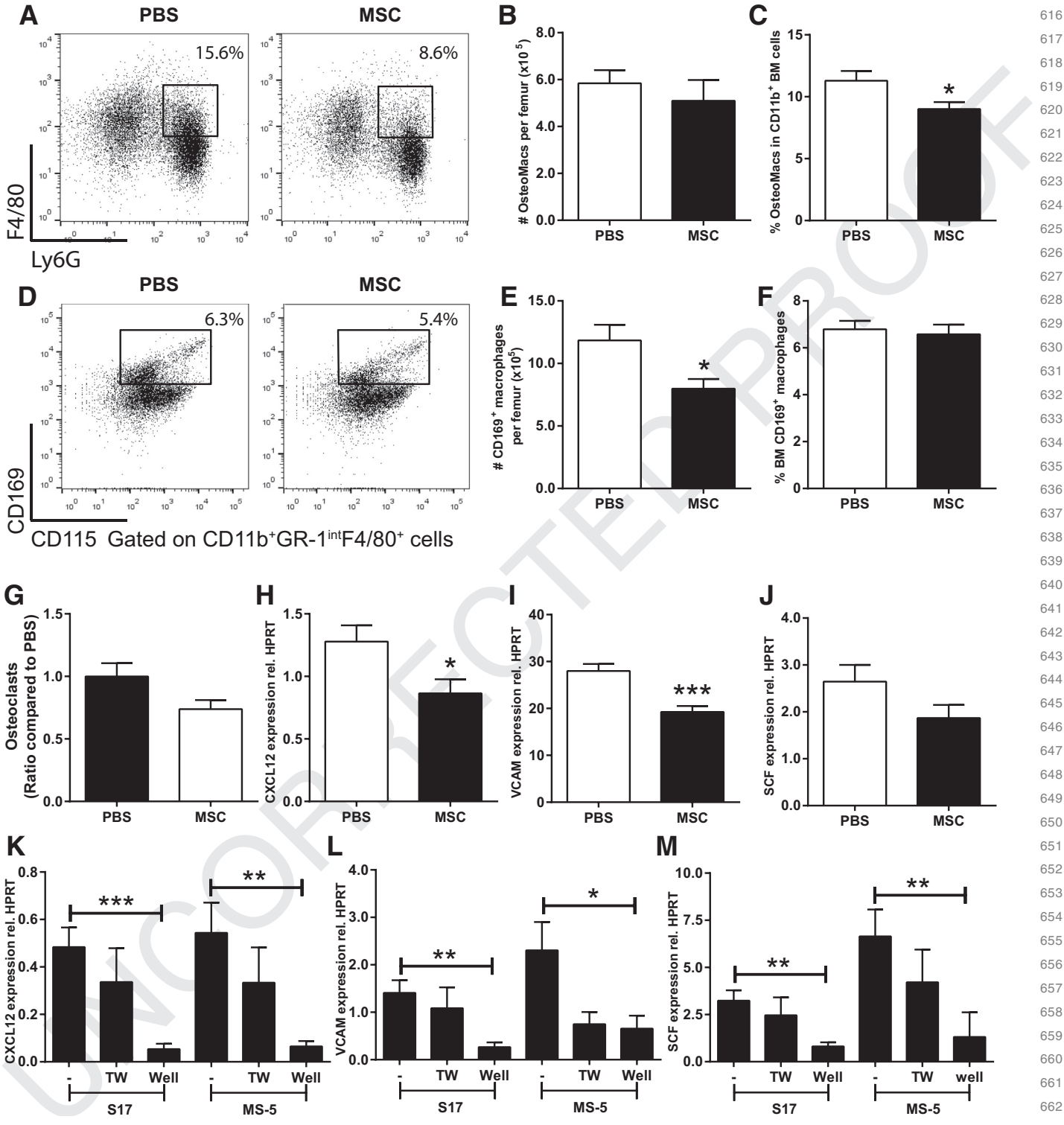

Figure 2. MSC administration induces downregulation of niche factors in the BM. (A–C) Osteomacs ($n = 12$), (D–F) CD169+ macrophages ($n = 6$), and (G) osteoclasts ($n = 10–13$) were analyzed on day 4 after 3 consecutive days of PBS or MSC administration. Relative RNA expression for (H) *Cxcl12*, (I) *Vcam*, and (J) *Scf* was determined in bone-lining cells after PBS or MSC administration and are depicted as the relative expression compared with the household gene HPRT ($n = 11–15$ from five separate experiments). (K–M) Stromal cells downregulate (K) *Cxcl12*, (L) *Vcam*, and (M) *Scf* upon cell–cell contact with RAW264.7 macrophages. RAW264.7 cells are cocultured with S17 or MS-5 stromal cells either in a Transwell (TW) or in direct cell–cell contact (Well; $n = 4–11$ from two to five separate experiments). Data are depicted as mean ± standard error of the mean. *$p < 0.05$, **$p < 0.005$, ***$p < 0.0005$ all compared with PBS.

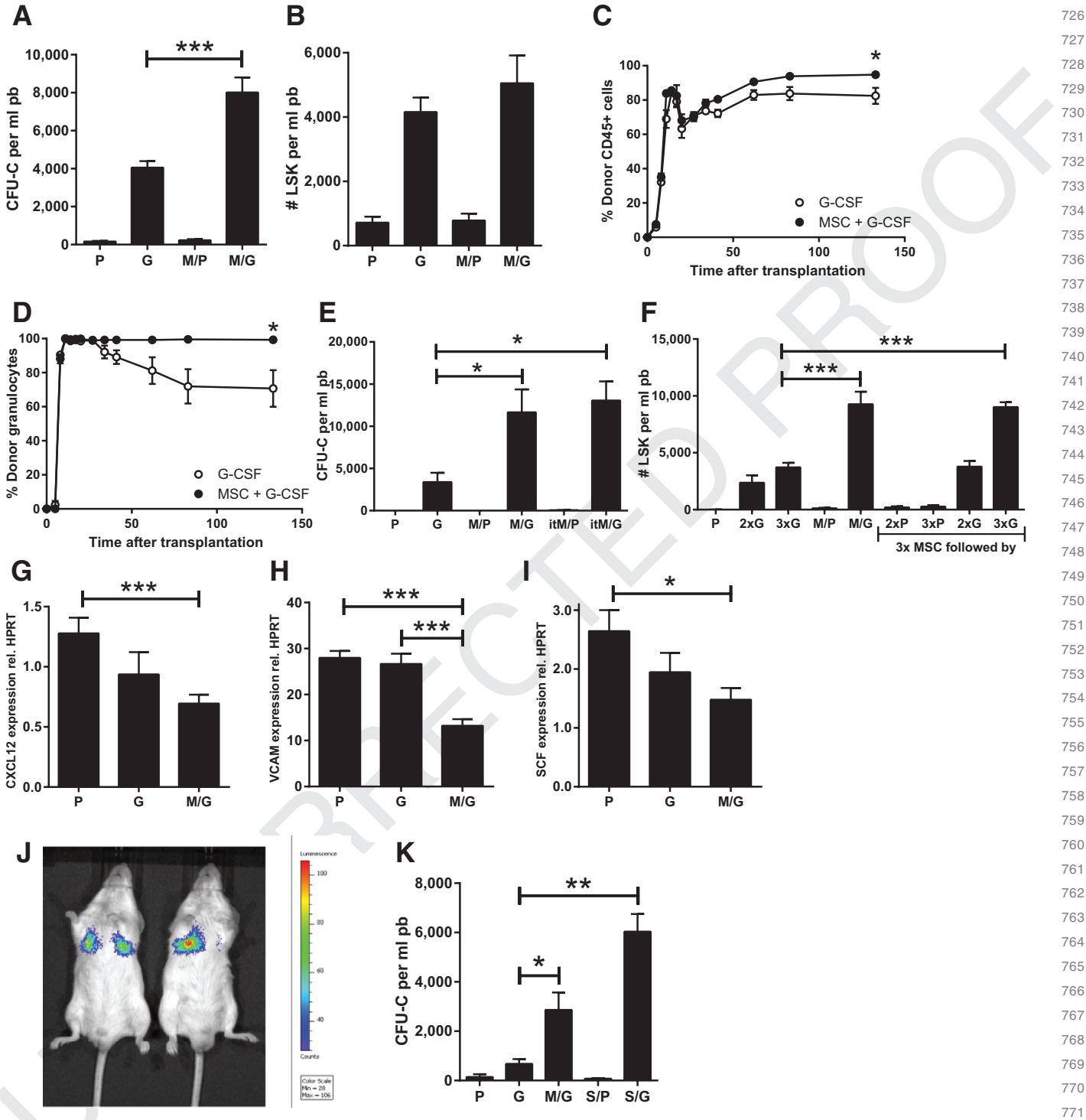

Figure 3. MSCs enhance G-CSF-induced HSPC mobilization through a soluble factor. (A) MSCs (M) were administered intravenously for 3 days at a dose of 200×10^3 cells per day to recipients that were simultaneously mobilized with G-CSF (G) (10 μg per day intraperitoneally for 3 days) or PBS (P) as a control ($n = 16-30$ per group). (B) The absolute number of LSK cells in the PB was analyzed using flow cytometry ($n = 8-11$ per group). (C) Equal numbers of PB cells obtained from G-CSF- or MSC + G-CSF-mobilized donors were transplanted into lethally irradiated recipients and donor chimerism for (C) total leukocytes and (D) granulocytes was assessed ($n = 10$ per group). (E) IFN-γ- and TNF-α-stimulated MSCs enhance G-CSF mobilization at levels similar to unstimulated MSCs. (F) MSC administration before G-CSF-induced mobilization enhances HSPC mobilization significantly. MSCs were administered intravenously for 3 days at a dose of 200×10^3 cells per day to recipients, followed by G-CSF administration on subsequent days (10 μg per day intraperitoneally for 2 or 3 days) or PBS as a control ($n = 3-6$ from two independent experiments). (G–I) Relative RNA expression for (G) *Cxcl12*, (H) *Vcam*, and (I) *Scf* was determined in bone-lining cells after G-CSF or MSC + G-CSF administration and depicted as relative expression compared with the household gene HPRT ($n = 10-14$ from five

administration coincided with increased levels of the osteoclast inhibitor OPG in the BM extracellular fluid ($p = 0.07$), whereas the levels of M-CSF remained unchanged (Supplementary Figures E2A and E2C, online only, available at www.exphem.org).

It has been reported that depletion of BM macrophages in vivo results in downregulation of *Cxcl12*, *Vcam, Ang-1*, and *Scf* [13–15]. Similarly, after MSC administration, the expression of *Cxcl12* and *Vcam* was decreased significantly in endosteal cells, whereas a modest decrease in *Scf* expression was observed (Figures 2H–2J).

To further study the effect of macrophages on gene expression in stromal cells, in vitro culture experiments were performed in which cells of the immortalized macrophage cell line RAW264.7 were incubated with either S17 or MS-5 stromal cells. Cultures were performed in a Transwell setting to investigate the effect of secreted factors or cell–cell contact. Next, gene expression was assessed. Direct cell–cell contact between RAW264.7 and stromal cells downregulated the expression of *Cxcl12*, *Vcam* and *Scf* significantly compared with S17 and MS-5 cultured in the absence of RAW264.7 cells. Factors secreted by RAW264.7 cells that were cultured in a Transwell only mildly affected the expression of *Cxcl12*, *Vcam*, and *Scf* (Figures 2K–2M).

Not only macrophages, but also B lymphocytes, were decreased significantly in the BM and PB after MSC administration (Supplementary Figures E2D–E2F, online only, available at www.exphem.org). This decrease coincided with a significant reduction in *IL-7* expression in endosteal cells. Given the crucial role of IL-7 in B lymphopoiesis [26], these results suggest that MSC administration may impair B lymphopoiesis in the BM.

MSCs enhance G-CSF-induced HSPC mobilization

The depletion of macrophages and the downregulation of *Cxcl12*, *Vcam*, and *Scf* observed after MSC administration have been reported to also occur during G-CSF-induced HSPC mobilization [14,27]. Therefore, we hypothesized that MSC administration may affect G-CSF-induced HSPC mobilization. To investigate this, MSCs were administered for 3 days to mice that were simultaneously mobilized with G-CSF. MSCs and G-CSF co-injection induced a twofold increase in HSPC mobilization compared with G-CSF administration alone, whereas administration of MSCs alone did not induce HSPC migration (Figure 3A). This effect was specific for MSCs because co-injection of splenocytes and G-CSF did not enhance HSPC mobilization (Supplementary Figure E3A, online only, available at www.exphem.org). A modest increase in LSK cells was observed in the PB (Figure 3B). To investigate whether MSCs and G-CSF coadministration increased the number of long-term repopulating HSCs in the PB, equal numbers of PB cells obtained after coinjection of MSCs and G-CSF or after G-CSF administration alone were transplanted into lethally irradiated recipient mice. Recipients of PB obtained from MSC- and G-CSF-mobilized donors showed significantly higher levels of donor leukocytes and granulocytes up to 19 weeks after transplantation compared with recipients of G-CSF-mobilized PB (Figures 3C and 3D). This indicates that co-administration of MSCs and G-CSF enhanced the mobilization of HSCs with long-term repopulating ability compared with G-CSF alone.

It has been shown previously that the immunomodulatory capacity of MSCs is enhanced in an inflammatory environment [25]. To determine whether exposure to inflammatory cytokines further enhances the capacity of MSCs to increase G-CSF-induced HSPC mobilization, MSCs were stimulated with IFN-γ and TNF-α before co-administration with G-CSF. IFN-γ- and TNF-α-stimulated MSCs indeed enhanced G-CSF mobilization, but cytokine-stimulated MSCs did not further enhance this effect compared with unstimulated MSCs (Figure 3E).

The effect that MSCs exert on the HSC niche seems to be independent of the effect established by G-CSF because administration of MSCs 3 days before G-CSF administration induced the same enhancement of G-CSF-induced mobilization as simultaneous MSCs and G-CSF administration (Figure 3F). In addition, administration of MSCs does not increase the levels of neutrophil elastase in the BM ($p = 0.28$; Supplementary Figure E3B, online only, available at www.exphem.org). A direct effect of G-CSF on MSCs can be excluded because MSCs do not express the G-CSF receptor (Supplementary Figure E3C, online only, available at www.exphem.org). Because osteoclasts were decreased upon MSC administration in combination with an increase in OPG (Figure 2G and Supplementary Figure E2A, online only, available at www.exphem.org), we assessed whether administration of OPG would enhance G-CSF-induced HSPC mobilization. However, no effect of OPG on G-CSF-induced mobilization was observed (Supplementary Figure E2B, online only, available at www.exphem.org). To investigate the effect of MSC and G-CSF co-administration on niche

separate experiments). (J) MSCs are trapped in the lung vasculature upon intravenous administration. Firefly luciferase-transduced MSCs were administered for 3 days. At day 4, MSCs were visualized by administration of luciferin followed by bioluminescence imaging. (K) Simultaneous administration of G-CSF and serum-free culture supernatant (S) enhances G-CSF-induced HSPC mobilization ($n = 5$ per group). Data are depicted as means ± standard error of the mean. *$p < 0.05$, **$p < 0.01$, ***$p < 0.001$.

genes, the expression of *Cxcl12*, *Vcam*, and *Scf* was assessed in endosteal cells. As expected, the expression of these genes was decreased after G-CSF administration. Moreover, co-administration of MSCs and G-CSF further downregulated the expression of these genes (Figures 3G–3I).

MSCs enhance G-CSF-induced mobilization through a soluble factor

To investigate the fate of MSCs upon intravenous administration, MSCs transduced with a lentiviral construct containing *SFFV-DsR-Fluc* were administered for 3 days and visualized by luciferin. Upon intravenous administration, MSCs migrated toward the lungs. No MSC migration to other locations was observed. This may be due to the sensitivity of the technique because a minimum of 5000 MSCs is required to obtain a signal that is distinguishable from background [21]. However, these results are consistent with previous observations [19].

Because no MSC migration toward the BM was observed, we hypothesized that, upon entrapment in the lungs, MSCs secrete soluble factors that in turn affect the HSC niche and enhance G-CSF-induced HSPC mobilization. Therefore, MSC culture supernatant was administered to recipients that were simultaneously mobilized with G-CSF. Coadministration of MSC culture supernatant and G-CSF enhanced G-CSF-induced mobilization significantly, whereas administration of culture supernatant alone did not affect HSPC migration toward the PB (Figure 3K).

MSC-derived EVs enhance G-CSF induced HSPC mobilization

MSCs have been reported to secrete EVs [20]. To investigate whether EVs are the supernatant-derived factor that enhanced G-CSF-induced HSPC mobilization, EVs derived from 2×10^6 to 0.2×10^6 MSCs were administered intravenously for 3 days to recipients that were simultaneously mobilized with G-CSF. Co-administration of EVs and G-CSF induced HSPC mobilization at similar levels as co-injection of MSCs and G-CSF (Figure 4A). Moreover, administration of MSC-derived EVs enhanced the cell cycle activity of LSK cells and downregulated the expression of *Cxcl12*, *Vcam*, and *Scf* similar to MSC administration (Figures 4B–4E). Previously, it has been shown that MSCs-derived EVs migrate to the BM [28]. To investigate which BM cells were able to engulf MSC-derived EVs, BM cells were incubated with PKH26-labeled EVs for 4 hours and the $PKH26^+$ cells were identified. Approximately 28% of the $CD45^+$ BM cells were able to engulf MSC-derived EVs (Figure 4F). Because >59% of the monocytic cells engulfed EVs (Figure 4F), we further investigated the phenotype of the EV^{POS} monocytic cells. EV^{POS} monocytic cells expressed F4/80, CD68, and MERTK at higher levels than EV^{NEG} monocytic cells. In addition, approximately 50% of the EV^{POS} cells expressed the M-CSF receptor (CD115; Figures 4G–4J). This indicates that macrophages are the main EV-engulfing population in the BM.

Discussion

MSCs are a cellular component of the HSC niche and play a major role in the maintenance of HSCs in the BM [1,2]. In addition, in an experimental transplantation model, coadministration of MSCs and HSPCs has a beneficial effect on HSC engraftment and hematopoietic recovery [18,19]. This suggests that MSCs are capable of influencing the HSC niche, leading to changes that result in altered HSC homeostasis.

Here, we show that MSC administration indeed affects the HSC niche, as well as the BM hematopoietic compartment. Upon MSC administration, HSC numbers in the BM were decreased, coinciding with increased HSC cell-cycling activity. Furthermore, MSC administration induced a decrease in BM macrophage subsets and concomitant downregulation of *Cxcl12*, *Vcam*, and *Scf* expression in endosteal cells. Previous studies have shown that BM macrophages have a regulatory role in hematopoiesis and in the HSC niche [29]. Furthermore, depletion of osteal macrophages and a downregulation of *Cxcl12*, *Scf*, and *Ang-1* mRNA is also observed during G-CSF-induced HSPC mobilization [14]. In steady state, macrophages regulate granulopoiesis and induce HSPC egress from the BM through circadian regulation of *Cxcl12* in stromal cells [30]. The decrease in Cxcl12 expression and HSPC egress is preceded by the downregulation of liver X receptor (LXR)–target gene downregulation in macrophages [30]. Depletion of BM macrophages results in downregulation of *Cxcl12*, *Vcam*, and *Scf*, increased HSC proliferation and HSPC mobilization [13–15,31]. Together, these previous studies and our data suggest that HSC-retaining factors in stromal cells are decreased due to macrophage depletion upon MSC administration and that increased HSPC cycling and mobilization may be a direct result of these events. This effect was specific for MSCs because co-injection of splenocytes and G-CSF did not enhance HSPC mobilization.

To study the interaction between macrophages and stromal cells, we performed in vitro experiments in which RAW264.7 macrophages were co-cultured with stromal cells. Cell–cell contact between RAW264.7 and stromal cells downregulated *Cxcl12*, *Vcam*, and *Scf* expression in stromal cells, whereas soluble factors secreted by RAW264.7 macrophages minimally influenced the expression of HSC-supporting genes. This

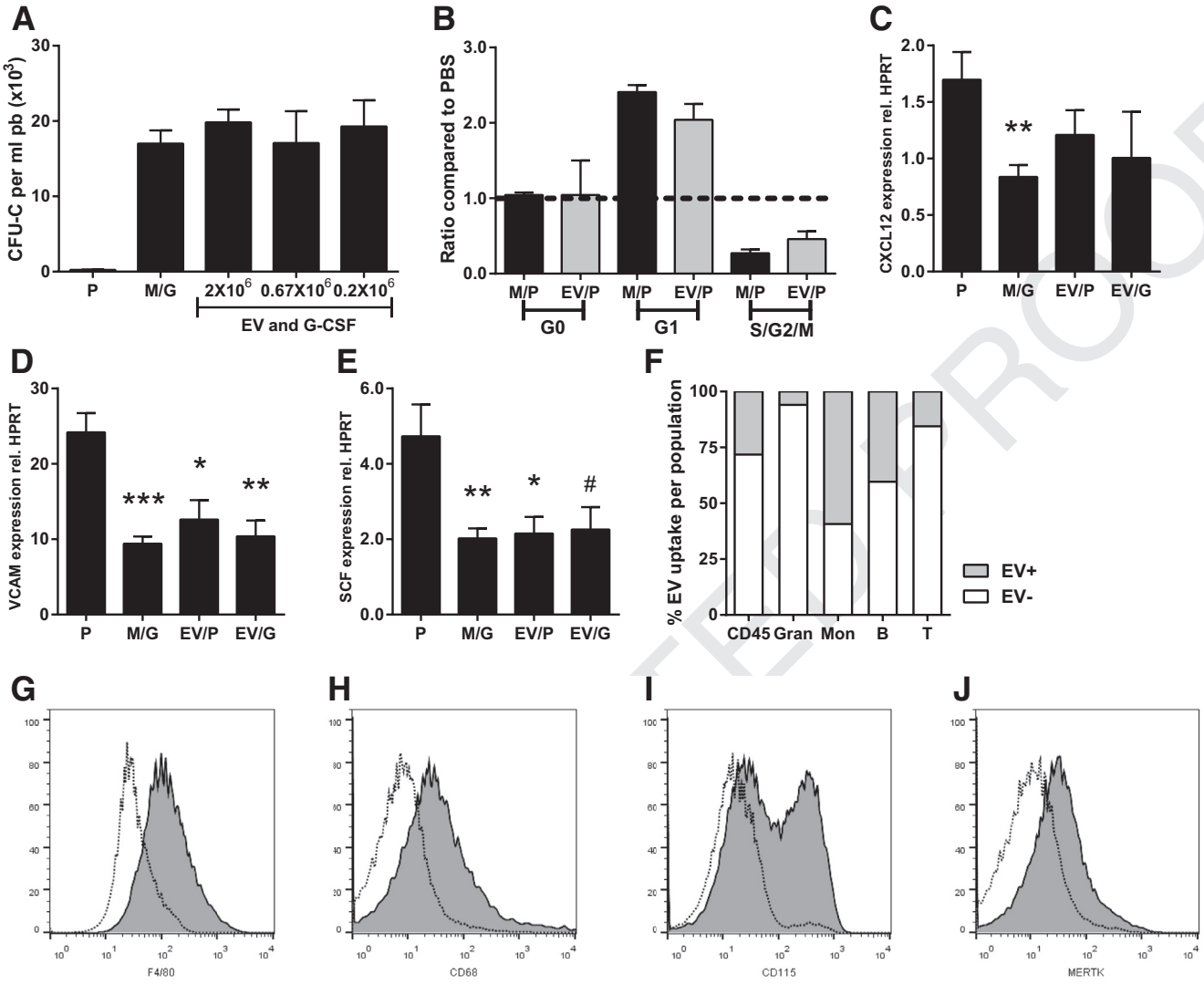

Figure 4. MSC-derived EVs enhance G-CSF-induced mobilization. (A) MSCs (M) or EVs derived from 2×10^6 to 0.2×10^6 MSCs were administered intravenously for 3 days to recipients that were simultaneously mobilized with G-CSF (G) or PBS (P) as a control ($n = 5-9$ per group). (B) Cell cycle activity of LSK cells was analyzed using a Ki67/DAPI staining. The frequencies of LSK cells in G_0, G_1, or $S/G_2/M$ phage was determined and related to PBS controls ($n = 4-6$ per group). (C–E) Relative RNA expression for (C) CXCL12, (D) VCAM, and (E) SCF was determined in bone-lining cells after MSC (M) or EV administration for 3 days to recipients that were simultaneously mobilized with G-CSF (G) or PBS (P) as a control. Gene expression is depicted as relative expression compared with the household gene HPRT ($n = 3-6$). Significance is indicated compared with p (#$p = 0.055$). (F) PKH26-labeled EV are primarily taken up by monocytes. The percentage of $CD45^+$ BM cells, granulocytes (Gran), monocytes (Mon), B cells (B), and T cells (T) that have taken up EVs are depicted within the total cell population. (G,H) Upon EV uptake, monocytes upregulate (G) F4/80, (H) CD68, (I) CD115, and (J) MERTK (data obtained from one experiment). EV^{neg} cells are depicted as a dotted line, EV^{pos} cells are depicted as filled histograms. Data are depicted as means ± standard error of the mean. *$p < 0.05$, **$p < 0.01$, ***$p < 0.001$.

further strengthens the evidence for a regulatory role of macrophages in the stem cell niche and indicates that cell–cell contact between stromal cells and macrophages is required for the downregulation of these factors.

When MSCs were co-administered with G-CSF, HSPC mobilization was enhanced significantly, indicating that the HSC niche is altered as a result of MSC injection. Because these MSCs are trapped in the lungs upon administration, it is conceivable that the observed increased mobilization is induced by a secreted factor. We considered that EVs secreted by MSCs could play such a role and therefore we embarked on experiments in which we coadministered MSCs or MSC-derived EVs and G-CSF. Indeed, coinjection of EVs and G-CSF induced HSPC mobilization at similar levels as MSCs and G-CSF. Coadministration of MSCs or MSC-derived EVs and G-CSF further downregulated the

expression of *Cxcl12*, *Vcam*, and *Scf* in endosteal cells compared with injection of either G-CSF or MSCs alone. Moreover, the events induced by MSC administration are independent of the events induced by G-CSF because sequential administration of MSCs and G-CSF also enhanced HSPC mobilization.

We show here that, in vitro, MSC-derived EVs are engulfed by F4/80$^+$MERTK$^+$CD68$^+$ BM-derived macrophages. Previously, it has been shown that CD68$^+$ cells that express the G-CSF-receptor mediate G-CSF-induced HSPC mobilization [32]. We therefore propose that, in vivo, MSC-derived EVs negatively affect this macrophage population, leading to downregulation of HSC-retaining factors in the niche. This, in turn, induces a permissive state in the BM that allows for significantly enhanced HSPC mobilization when G-CSF is administered.

In recent years, studies have indicated that MSC-derived EVs are associated with a variety of hematopoietic disorders [33–35]. MSC-derived EVs are also thought to play a supporting role in tissue homeostasis and to influence responses to injury and infection [20,36]. EVs secreted by murine or human MSCs, are able to inhibit radiation-induced apoptosis of the murine hematopoietic cell line FDC-P1 [28]. In addition, administration of MSC-derived EVs resulted in long-term survival in lethally irradiated mice due to a direct radioprotective effect on HSCs [37].

In conclusion, both MSCs and MSC-derived EVs alter the stem cell niche and induce a permissive state in the BM. This state is characterized by macrophage depletion and downregulation of niche factors, thereby resulting in enhanced HSPC mobilization upon G-CSF administration. Further studies will be required to identify the exact EV component(s) that is responsible for the effects on the stem cell niche. Identification of this factor(s) may potentially lead to novel HSPC mobilization strategies.

Acknowledgements

This work was supported grants from the Wijnand M. Pon Foundation and the Dutch government to the Netherlands Institute for Regenerative Medicine (NIRM FES0908).

Conflict of interest disclosure

The authors declare no competing financial interests.

References

1. Morrison SJ, Scadden DT. The bone marrow niche for haematopoietic stem cells. Nature. 2014;505:327–334.
2. van Pel M, Fibbe WE, Schepers K. The human and murine hematopoietic stem cell niches: are they comparable? Ann N Y Acad Sci. 2016;1370:55–64.
3. Kunisaki Y, Bruns I, Scheiermann C, et al. Arteriolar niches maintain haematopoietic stem cell quiescence. Nature. 2013;502:637–643.
4. Mendez-Ferrer S, Michurina TV, Ferraro F, et al. Mesenchymal and haematopoietic stem cells form a unique bone marrow niche. Nature. 2010;466:829–834.
5. Pinho S, Lacombe J, Hanoun M, et al. PDGFRalpha and CD51 mark human nestin+ sphere-forming mesenchymal stem cells capable of hematopoietic progenitor cell expansion. J Exp Med. 2013;210:1351–1367.
6. Zhou BO, Yue R, Murphy MM, Peyer JG, Morrison SJ. Leptin-receptor-expressing mesenchymal stromal cells represent the main source of bone formed by adult bone marrow. Cell Stem Cell. 2014;15:154–168.
7. Ding L, Morrison SJ. Haematopoietic stem cells and early lymphoid progenitors occupy distinct bone marrow niches. Nature. 2013;495:231–235.
8. Ding L, Saunders TL, Enikolopov G, Morrison SJ. Endothelial and perivascular cells maintain haematopoietic stem cells. Nature. 2012;481:457–462.
9. Winkler IG, Barbier V, Wadley R, Zannettino A, Williams S, Levesque JP. Positioning of bone marrow hematopoietic and stromal cells relative to blood flow in vivo: Serially reconstituting hematopoietic stem cells reside in distinct non-perfused niches. Blood. 2010;116:375–385.
10. Greenbaum A, Hsu YM, Day RB, et al. CXCL12 in early mesenchymal progenitors is required for haematopoietic stem-cell maintenance. Nature. 2013;495:227–230.
11. Oguro H, Ding L, Morrison SJ. SLAM family markers resolve functionally distinct subpopulations of hematopoietic stem cells and multipotent progenitors. Cell Stem Cell. 2013;13:102–116.
12. Pruijt JF, van Kooyk Y, Figdor CG, Willemze R, Fibbe WE. Murine hematopoietic progenitor cells with colony-forming or radioprotective capacity lack expression of the beta 2-integrin LFA-1. Blood. 1999;93:107–112.
13. Chang MK, Raggatt LJ, Alexander KA, et al. Osteal tissue macrophages are intercalated throughout human and mouse bone lining tissues and regulate osteoblast function in vitro and in vivo. J Immunol. 2008;181:1232–1244.
14. Winkler IG, Sims NA, Pettit AR, et al. Bone marrow macrophages maintain hematopoietic stem cell (HSCs) niches and their depletion mobilizes HSCss. Blood. 2010;116:4815–4828.
15. Chow A, Lucas D, Hidalgo A, et al. Bone marrow CD169+ macrophages promote the retention of hematopoietic stem and progenitor cells in the mesenchymal stem cell niche. J Exp Med. 2011;208:261–271.
16. Kuiperij HB, van Pel M, de Rooij KE, Hoeben RC, Fibbe WE. Serpina1 (alpha1-AT) is synthesized in the osteoblastic stem cell niche. Exp Hematol. 2009;37:641–647.
17. Winkler IG, Hendy J, Coughlin P, Horvath A, Levesque JP. Serine protease inhibitors serpina1 and serpina3 are down-regulated in bone marrow during hematopoietic progenitor mobilization. J Exp Med. 2005;201:1077–1088.
18. van der Garde M, van Pel M, Millan Rivero JE, et al. Direct comparison of Wharton's jelly and bone marrow-derived mesenchymal stromal cells to enhance engraftment of cord blood CD34(+) transplants. Stem Cells Dev. 2015;24:2649–2659.
19. Noort WA, Kruisselbrink AB, in't Anker PS, et al. Mesenchymal stem cells promote engraftment of human umbilical cord blood-derived CD34(+) cells in NOD/SCID mice. Exp Hematol. 2002;30:870–878.
20. Lai RC, Yeo RW, Lim SK. Mesenchymal stem cell exosomes. Semin Cell Dev Biol. 2015;40:82–88.
21. Perez-Galarza J, Carlotti F, Rabelink MJ, et al. Optimizing reporter constructs for in vivo bioluminescence imaging of

Q5

interferon-gamma stimulated mesenchymal stromal cells. Exp Hematol. 2014;42:793–803. e1.
22. de Kruijf EJ, Hagoort H, Velders GA, Fibbe WE, van PM. Hematopoietic stem and progenitor cells are differentially mobilized depending on the duration of Flt3-ligand administration. Haematologica. 2010;95:1061–1067.
23. Melief SM, Schrama E, Brugman MH, et al. Multipotent stromal cells induce human regulatory T cells through a novel pathway involving skewing of monocytes toward anti-inflammatory macrophages. Stem Cells. 2013;31:1980–1991.
24. Maggini J, Mirkin G, Bognanni I, et al. Mouse bone marrow-derived mesenchymal stromal cells turn activated macrophages into a regulatory-like profile. PLoS One. 2010;5:e9252.
25. Bernardo ME, Fibbe WE. Mesenchymal stromal cells: sensors and switchers of inflammation. Cell Stem Cell. 2013;13:392–402.
26. Clark MR, Mandal M, Ochiai K, Singh H. Orchestrating B cell lymphopoiesis through interplay of IL-7 receptor and pre-B cell receptor signalling. Nat Rev Immunol. 2014;14:69–80.
27. Winkler IG, Pettit AR, Raggatt LJ, et al. Hematopoietic stem cell mobilizing agents G-CSF, cyclophosphamide or AMD3100 have distinct mechanisms of action on bone marrow HSCs niches and bone formation. Leukemia. 2012;26:1594–1601.
28. Wen S, Dooner M, Cheng Y, et al. Mesenchymal stromal cell-derived extracellular vesicles rescue radiation damage to murine marrow hematopoietic cells. Leukemia. 2016;30:2221–2231.
29. McCabe A, MacNamara KC. Macrophages: Key regulators of steady-state and demand-adapted hematopoiesis. Exp Hematol. 2016;44:213–222.
30. Casanova-Acebes M, Pitaval C, Weiss LA, et al. Rhythmic modulation of the hematopoietic niche through neutrophil clearance. Cell. 2013;153:1025–1035.
31. McCabe A, Zhang Y, Thai V, Jones M, Jordan MB, MacNamara KC. Macrophage-lineage cells negatively regulate the hematopoietic stem cell pool in response to interferon gamma at steady state and during infection. Stem Cells. 2015;33:2294–2305.
32. Christopher MJ, Rao M, Liu F, Woloszynek JR, Link DC. Expression of the G-CSF receptor in monocytic cells is sufficient to mediate hematopoietic progenitor mobilization by G-CSF in mice. J Exp Med. 2011;208:251–260.
33. Roccaro AM, Sacco A, Maiso P, et al. BM mesenchymal stromal cell-derived exosomes facilitate multiple myeloma progression. J Clin Invest. 2013;123:1542–1555.
34. Muntion S, Ramos TL, Diez-Campelo M, et al. Microvesicles from mesenchymal stromal cells are involved in HPC-microenvironment crosstalk in myelodysplastic patients. PLoS One. 2016;11:e0146722.
35. Viola S, Traer E, Huan J, et al. Alterations in acute myeloid leukaemia bone marrow stromal cell exosome content coincide with gains in tyrosine kinase inhibitor resistance. Br J Haematol. 2016;172:983–986.
36. Phinney DG, Pittenger MF. Concise review: MSCs-derived exosomes for cell-free therapy. Stem Cells. 2017;35:851–858.
37. Schoefinius JS, Brunswig-Spickenheier B, Speiseder T, Krebs S, Just U, Lange C. Mesenchymal stromal cell-derived extracellular vesicles provide long-term survival after total body irradiation without additional hematopoietic stem cell support. Stem Cells. 2017;35:2379–2389.

Supplementary Files

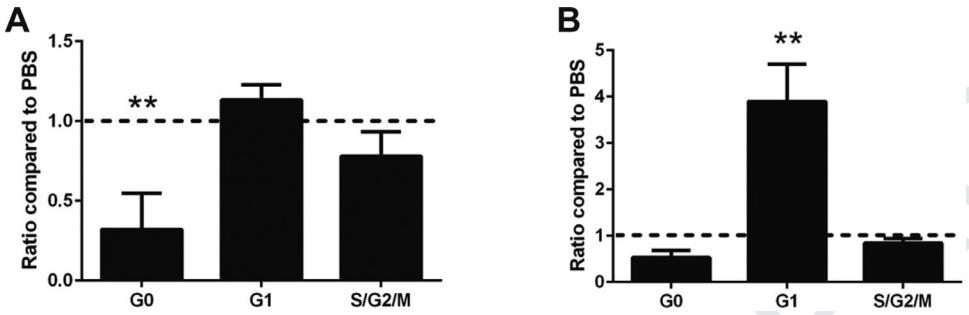

Supplementary Figure E1. MSC administration increases HSPC cell cycle activity. Following 3 days of intravenous MSC, femurs were isolated. Using a Ki67/DAPI staining, cell cycle activity of (A) HSC and (B) HPC/MPP was analyzed and related to PBS controls. Data are depicted as mean ± SEM, n=7 per group **p<0.01 compared to PBS.

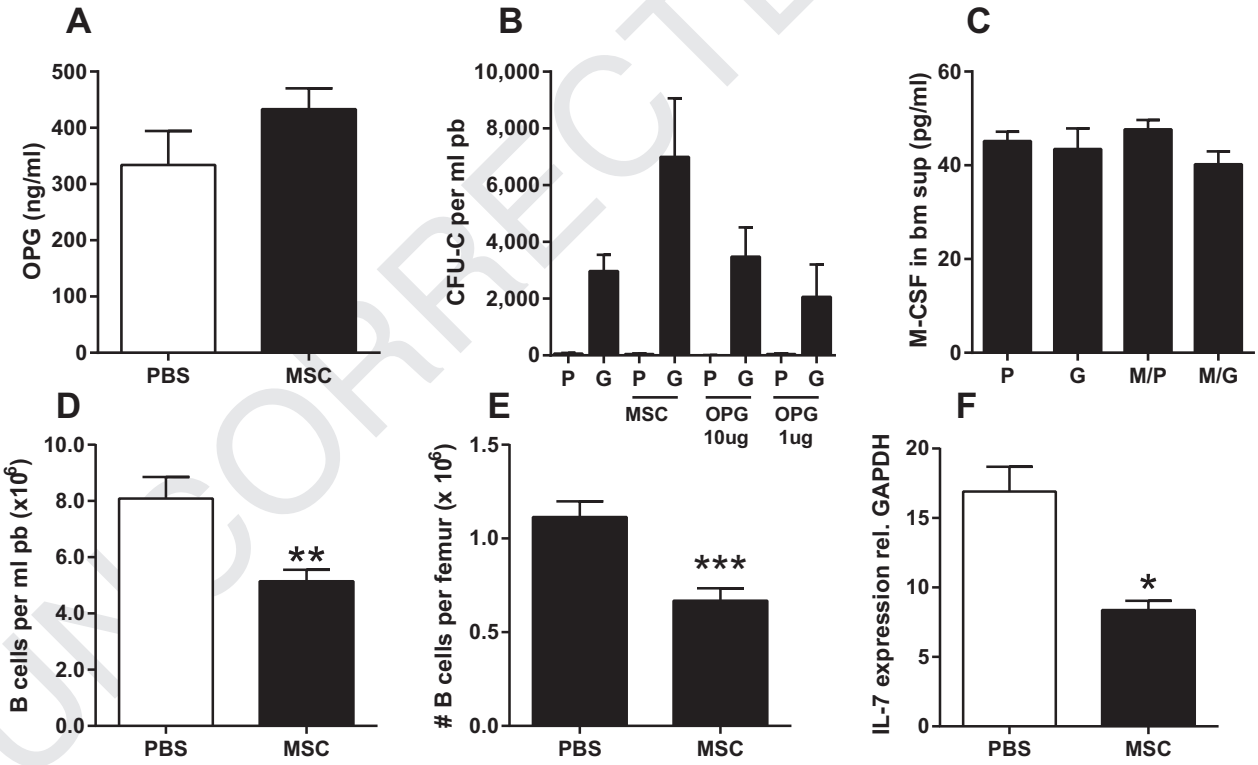

Supplementary Figure E2. Effect of MSC administration on the hematopoietic stem cell miroenvironment. Following 3 days of intravenous MSC or PBS administration (A) osteoprotegerin (OPG) levels were increased in bone marrow extracellular fluid upon MSC administration (n=3 per group). (B) OPG administration does not affect G-CSF-induced mobilization. OPG was administered at 10 μg or 1 μg per day for 3 days. At the same time points, PBS (P) or G-CSF (G) was administered; n=3-5 per group. (C) M-CSF (n=5-13) levels were determined in bone marrow extracellular fluid. Following 3 days of intravenous MSC or PBS administration B cells were significantly decreased in the (D) peripheral blood and (E) bone marrow (n=9-13). (F) This coincides with a decrease in *Il-7* expression in bone-lining cells. p<0.05, **p<0.01, ***p<0.001.

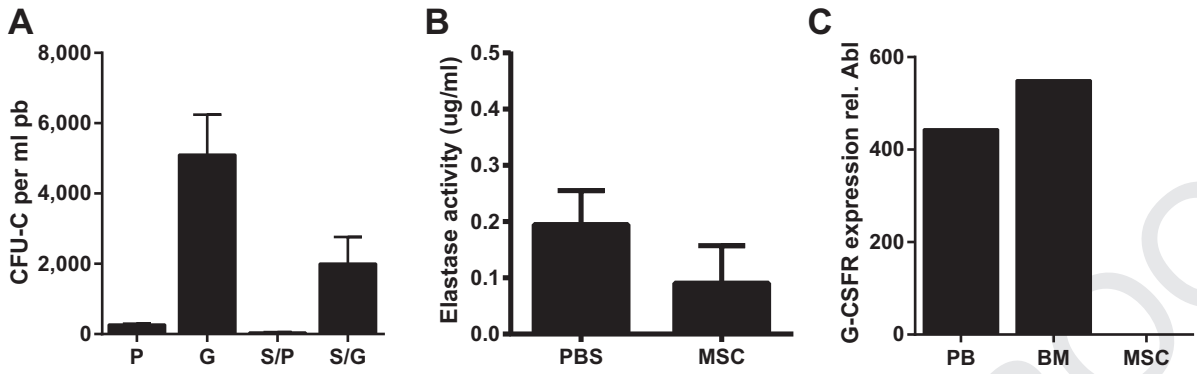

Supplementary Figure E3. (A) Splenocytes (S) were administered intravenously for 3 days at a dose of 200 x10^3 cells per day to recipients that were simultaneously mobilized with G-CSF (G; 10 μg per day intraperitoneally for 3 days) or PBS (P) as a control (n= 3 per group). Data are depicted as mean ± SEM. (B) Administration of MSC does not affect elastase levels in the bone marrow. Bone marrow extracellular extracts were obtained by flushing femurs with 250 μl cold PBS. The cell suspension was centrifuged at 2,300 g for 5 minutes and the supernatant was stored at -20 °C. Elastase activity was determined using the chromogenic substrate N-Succinyl-L-Ala-Ala-Ala-P-nitroanilide (Sigma, Zwijndrecht, The Netherlands). Data are depicted as mean ± SEM (n=5-6) (C) *Csf3R* expression was assessed on peripheral blood cells (PB), bone marrow cells (BM) or MSC and depicted as relative expression compared to the household gene *Abl* (mean of triplicates are indicated).